Hindawi
Shock and Vibration
Volume 2023, Article ID 5546795, 11 pages
https://doi.org/10.1155/2023/5546795

Research Article

Research and Application of Rock Burst Hazard Assessment of the Working Face Based on the CF-TOPSIS Method

Feng Zhu,[1,2,3,4] Haowei Song,[1] Bingxiang Huang,[2] Binxin Hu,[1] Siqi Li,[5] Guangdong Song,[1] Hua Zhang,[1] Tongyu Liu,[1,3] and Fuwu Ma[4,6]

[1]*Laser Research Institute, Qilu University of Technology (Shandong Academy of Sciences), Jinan 250014, China*
[2]*State Key Laboratory of Coal Resources and Safe Mining, China University of Mining and Technology, Xuzhou 221116, China*
[3]*Jining Anran Intelligent Technology Co. Ltd, Jining 272000, China*
[4]*Engineering Laboratory of Deep Mine Rock Burst Disaster Assessment, Jinan 250102, China*
[5]*Shanxi Lu'an Environmental Protection Energy Development Co., Ltd., Wuyang Coal Mine, Changzhi 046200, China*
[6]*Shandong Province Research Institute of Coal Geology Planning and Exploration, Jinan 250102, China*

Correspondence should be addressed to Haowei Song; 2282826154@qq.com

Received 30 March 2023; Revised 28 May 2023; Accepted 6 June 2023; Published 22 June 2023

Academic Editor: Pengfei Wang

Coal mining activities have intensified, and underground mining depths have increased, posing significant challenges for mitigating rock burst hazard. To address this issue, this paper proposes an improved comprehensive weighting prediction (CF-TOPSIS) method that predicts weight and grade indices for rock burst evaluation. The study introduces a novel variable coefficient method to optimize the conflict response problem and employs correlation forward and other techniques to minimize errors caused by large data differences. Based on these, the CRITIC objective weight algorithm model is established, and FAHP is used to optimize weighting factors to make the index weight of rock burst more reasonable, thus enhancing the accuracy of hazard assessment for working faces. Results from engineering examples show that the prediction results combined with field drill cutting methods and microseismic monitoring data verify the accuracy of the proposed method, indicating its feasibility and effectiveness in predicting rock burst hazard in underground coal mines.

1. Introduction

Coal is a pivotal source of energy in China's energy portfolio [1]. However, with the gradual exhaustion of shallow coal seams, deep mining has become increasingly prevalent, leading to a higher probability of deep rock bursts [2, 3]. Thus, to ensure the safety of coal mining operations, accurate and effective prediction of rock bursts in deep mining must be based on scientific and rigorous principles [4].

Numerous scholars have conducted extensive research on predicting rock bursts [5]. Their proposed measures can be categorized into mine-wide prediction (intelligent hazard-level judgement), regional prediction (utilizing three spatialtemporal monitoring methods), and local prediction (employing a multiparameter monitoring and early warning index system for rock bursts) [6–10]. Given the complexity of factors contributing to rock bursts, evaluating the level of rock bursts in mines can be challenging. Wu et al. [11] judged rock burst hazard levels by utilizing a rock comprehensive prediction model, which involved determining the hazard index of rock bursts. To predict the static properties of coal and rock mass, Jiang et al. [12] developed a possibility index diagnosis method that considers mining stress and the burst tendency of coal seams as primary indices. Zhu and Zhang [13] introduced the Lagrange function to optimize the decision model and address the issue of determining the weight of rock burst disaster system evaluation models. Han et al. [14] established the division method of geological dynamic zones, incorporating fault structure and coal rock characteristics to enable accurate coal mine prediction. Based on the cloud model and D-S theory, Chen [15] evaluated the hazard of rock burst, while

Cai et al. [16] further developed the spatiotemporal forecasting method for rock bursts using multidimensional microseismic information. To address the challenge of predicting dynamic disasters caused by various factors and the heterogeneity of coal and rock in mining operations, Meng et al. [17] studied the general patterns and hazard control factors of rock bursts. Additionally, in regional prediction methods that involve "strong time and space" considerations, several techniques such as the generalized artificial neural network [18], particle swarm optimization KNN, cloud model, and decision tree [19, 20] have yielded promising results in rock burst prediction. However, each prediction method has its limitations. For instance, the convergence speed of intelligent algorithms like generalized neural networks may be slow. Decision tree algorithms can be prone to overfitting and may overlook correlations, while the analytic hierarchy process may exhibit strong subjectivity. Similarly, the conventional objective weighting method may fail to account for interindicator correlations [21–25].

Given that rock bursts can be affected by numerous factors [26, 27], this study optimizes the correlation and conflict of CRITIC and constructs the CF comprehensive weight evaluation index through a combination of the FAHP's subjective weight approach [28]. The improved TOPSIS rock burst closeness evaluation and prediction model yields more accurate and reasonable predictions of rock burst grade. The accuracy of these predictions is verified through a practical example, highlighting the effectiveness of the proposed approach.

2. Comprehensive Weighted Prediction Model

Rock bursts occur due to the influence of multiple factors, and the rock burst of each factor on rock bursts can vary. As such, determining a reasonable comprehensive evaluation model for rock bursts and assessing the hazard level of the working face are of paramount importance.

2.1. Improved Objective Weighting Method. The entropy weight method (EWM) is an important means of reducing subjective factors in the evaluation process. However, EWM has limitations in reflecting the interrelationship between criteria, which may affect the accuracy of the evaluation results. To address this issue, a new approach called criteria importance through intercriteria correlation (CRITIC) was proposed by Diakoulaki in 1995. CRITIC serves to optimize the weighting procedure and improve the objectivity of the evaluation process by taking into account the interrelationship between criteria [29, 30]:

(1) The index data matrix $X = (x_{ij})_{m\times n}$ is established, and indicator types are unified.

$$\begin{cases} x_{ij} = x_{ij}^{(1)}, \\ x_{ij}^{(1)} = \max x_j - x_{ij}, \end{cases} \tag{1}$$

where x_{ij} is the original data of the influencing factors of rock burst and $x_{ij}^{(1)}$ is the positive value of the index.

(2) Standardized processing of forwarded matrices is

$$x_{ij}^{*} = \frac{x_{ij}^{*}}{\sqrt{\sum_{i=1}^{m} x_{ij}^{(1)^2}}}. \tag{2}$$

(3) The correlation coefficient between the influencing factors is obtained by the processed matrix.

There is a connection between the influencing factors, and the deviation product can well measure the degree of correlation between the two variables:

$$\xi_{ij} = \sum_{i=1}^{n} x_i - \frac{\overline{x}}{\sqrt{\sum_{i=1}^{n} \left(x_j - \overline{x}\right)^2 \sum_{i=1}^{n} \left(y_i - \overline{y}\right)^2}}. \tag{3}$$

ξ_{ij} indicates that $(i = 1, 2, 3\cdots n; j = 1, 2, 3\cdots n)$ is the correlation coefficient between the ith indicator and the jth indicator, and the value of ξ_{ij} is between (0, 1). The greater the value of ξ_{ij}, the greater the correlation between the two factors.

(4) The information amount of the comprehensive measurement index is as follows:

Information measure C_j is defined based on contrast strength and conflict concepts:

$$C_j = \sigma_j \sum_{i=1}^{n} 1 - \xi_{ij}, \tag{4}$$

where C_j represents the definition of information measure, σ_j represents variance, and ξ_{ij} represents the correlation coefficient.

In the present study, an optimized criteria importance through intercriteria correlation (CRITIC) approach is proposed to enhance the objectivity of weight determination. While Zhang and Xiao [31] proposed the use of CRITIC, this method has not been applied in the field of rock burst hazard assessment. The significant differences in influencing factors of rock burst pressure are addressed by optimizing the CRITIC approach in order to account for these differences. Due to the large variations in rock burst pressure influencing factors, the value of the consistency coefficient (C_j) may become too large, leading to errors in the determination of weight factors. The coefficient of the variation method is utilized to enhance the CRITIC approach and address errors stemming from excessively large C_j values. Furthermore, the method is optimized to accommodate situations where notable variations in indicator values pose challenges in implementing the coefficient of the variation approach:

$$\overline{x}_j = \frac{\left(x_{\max 1j} + x_{\max 2j}\right) - \left(x_{\min 1j} + x_{\min 2j}\right)}{2}, \tag{5}$$

$$v_i = \frac{\sigma_j}{\overline{x}_j}, \quad (j = 1, 2, \cdots, n), \tag{6}$$

where j is the number of index values and σ_j is the variance.

In Zhao et al. [32] evaluation of power quality classification, the $1 - \xi_{ij}$ value reflects the conflict between different evaluation indicators. However, when the relationship between indicators is negative, weighting may become disproportionately large. To address this issue and account for the conflicts among coefficient values, a positive conflict transformation method is introduced to optimize the weight determination process. By applying this approach, the issue of disproportionately large weights resulting from negative correlations between indicators is effectively mitigated:

$$C_j = v_j \sum_{i=1}^{n} 1 - \left|\xi_{ij}\right|, \tag{7}$$

where v_i is the introduced coefficient of variation and ξ_{ij} is the correlation coefficient.

(5) Calculation of the index weight of the information measure index is

$$w_{Aj} = \frac{C_j}{\sum_{j=1}^{n} C_j}, \tag{8}$$

where w_{Aj} represents the weight value of the index j.

2.2. Determining Subjective Weight by FAHP. The traditional AHP method fails to maintain consistency in thinking when facing multiple evaluation indicators. It is difficult to test the consistency of the judgment matrix, which fails to provide a strong scientific basis. In order to further optimize the reliability of the subjective weight, the author uses the fuzzy analytical hierarchy process (FAHP) to establish a multiobjective, multilevel structure of the subjective weight of the rock burst subjective decision model [33].

A number of experts with rich work experience compare and judge the two factors of rock burst, construct the judgment matrix $J = (a_{ij})_{n\times n}$, and calculate the average value of each a_{ij} obtained by many experts to obtain $A = (a_{ij})_{n\times n}$. The subjective weight w_{Bj} is obtained by summing the fuzzy judgment matrix A by rows and exchanging them mathematically:

$$\begin{cases} r_{ij} = \dfrac{r_i - r_j}{2n} + 0.5, \\ a_{ij} = r_{ij}. \end{cases} \tag{9}$$

The subjective factor weight calculation equation is as follows:

$$\begin{cases} w_{Bi} = \dfrac{1}{n} - \dfrac{1}{2a} + \dfrac{1}{an} \times \sum_{i=1}^{n} r_{ik}, \\ a = \dfrac{n-1}{2}. \end{cases} \tag{10}$$

2.3. CF-TOPSIS Regional Static Prediction before Mining. The technique for order preference by similarity to ideal solution (TOPSIS) can better describe the strength of multifactor comprehensive influence of rock burst without the objective function and test [34]. TOPSIS avoids errors caused by subjective factors in data and is often used for multiple indicators and evaluation units [35]. In this paper, through the optimized CF combination weight, according to the distance between the positive and negative ideal solutions, the rock burst pressure level and the working face to be measured are sorted to realize the prediction of the rock burst hazard level of the working face before rock burst pressure mining.

The optimized objective weight and the subjective weight are combined to obtain the CF comprehensive weight:

$$W_{AB} = \frac{\sqrt{w_{Aj} w_{Bj}}}{\sum_{j=1}^{n} \sqrt{w_{Aj} w_{Bj}}}, \tag{11}$$

where W_{AB} is the comprehensive index weight coefficient and w_{Aj} and w_{Bj} represent the values of the objective weight and subjective weight after optimization, respectively.

2.3.1. Original Judgment Matrix. The rock burst level scheme set is set as $G = G_1, G_2, \cdots, G_m$, and the index set to be evaluated is $e = \{e_1, e_2, \cdots, e_m\}$. The binary comparison decision matrix, as presented in equation (10), serves as a means of identifying the internal correlated significance of factors [36]. The evaluation index e_{ij} represents the jth evaluation index of the ith scheme.

The initial evaluation matrix is as follows:

$$G = \left(e_{ij}\right)_{m\times n} = \begin{bmatrix} e_{11} - \cdots & e_{1n} \\ \vdots - \ddots & \vdots \\ e_{m1} - \cdots & e_{mn} \end{bmatrix}. \tag{12}$$

2.3.2. Standardized Decision Matrix. The evaluation index can be divided into the consumption index and profitability index. For the consumption index, the smaller the value, the better. For the profitability index, the larger the value, the better. Because each evaluation index has different dimensions and units, it has no comparability, so e_{ij} is standardized to get the decision matrix $B = (b_{ij})_{m\times n}$:

$$B_{ij} = \begin{cases} b_{ij}^{*} = \dfrac{a_{ij}}{\sqrt{\sum_{i=1}^{m} a_{ij}^2}}, \\ b_{ij} = \left(\dfrac{1}{a_{ij}}\right) \sqrt{\sum_{i=1}^{m} \left(\dfrac{1}{a_{ij}}\right)^2} \end{cases}, \tag{13}$$

where b_{ij}^{*} is the profitability index and b_{ij} is the consumption index.

2.3.3. Weighted Standardized Decision Matrix. The weighted standardized decision matrix E is obtained by multiplying the column vector of matrix B with the total ranking weight W_n of the determined comprehensive weight index layer:

$$E = \left(e_{ij}\right)_{m\times n} = \begin{bmatrix} w_1 b_{11} - \cdots & w_n b_{1n} \\ \vdots - \ddots & \vdots \\ w_1 b_{m1} - \cdots & w_n b_{mn} \end{bmatrix}. \tag{14}$$

2.3.4. Close Degree Analysis. The positive ideal solution of the profitability index set l_1 is the maximum value of the row vector, the negative ideal solution is the minimum value of the row vector, and the value of the consumption index set l_2 is the opposite:

$$\begin{cases} E^{+} = \left\{\left(\max\limits_{n} w_n b_{mn} | m \in l_1\right), \left(\min\limits_{n} w_n b_{mn} | m \in l_2\right)\right\}, \\ E^{-} = \left\{\left(\min\limits_{n} w_n b_{mn} | m \in l_1\right), \left(\max\limits_{n} w_n b_{mn} | m \in l_2\right)\right\}, \end{cases} \tag{15}$$

where E^{+} and E^{-} are the positive ideal solution and the negative ideal solution, respectively. In order to better optimize the distance between the evaluation object and the ideal solution, the influence of each influencing factor on the rock burst of low pressure is different. The greater the weight, the greater the possibility of rock burst.

Zhu and Zhang [13] incorporated the weighting coefficients w_{AB} into the positive and negative ideal solutions to develop the CF-TOPSIS model. Through this approach, they were able to optimize the rock burst of the weight coefficients on the evaluation of the rock burst of ground pressure while also conducting proximity analysis. The deviation equation resulting from the weighting coefficients and the Euclidean distance of the ideal solutions were also examined:

$$\begin{cases} F_i^{+} = \sqrt{\sum\limits_{j=1}^{n} w_{AB}\left(e_{ij} - e_j^{+}\right)^2}, \\ F_i^{-} = \sqrt{\sum\limits_{j=1}^{n} w_{AB}\left(e_{ij} - e_j^{-}\right)^2}, \end{cases} \tag{16}$$

where e_i^{+} and e_i^{-} are the element corresponding to the positive and negative ideal solutions and F_i^{+} and F_i^{-} represent the distance between the positive and negative ideal solutions.

The calculation equation of closeness analysis is as follows:

$$H_i^{+} = \frac{F_i^{-}}{F_i^{+}} + F_i^{-}, \quad \left(0 \le H_i^{+} \le 1\right), \tag{17}$$

where H_i^{+} is the value of the closeness degree of the evaluation object, and the range is (0, 1), which reflects the degree of closeness of the evaluation object to the positive ideal solution.

The evaluation matrix is constructed by the close degree analysis of the TOPSIS method. The comprehensive evaluation result vector Q of the CF-TOPSIS model is calculated as follows:

$$Q = W \times H, \tag{18}$$

where Q is the comprehensive evaluation result vector, H is the evaluation matrix formed by the closeness degree between each evaluation object and the positive ideal solution, and W is the criterion layer weight calculated by the comprehensive weight method. The CF-TOPSIS comprehensive evaluation model is shown in Figure 1.

3. Comprehensive Prediction of Rock Burst Hazard in Working Face

3.1. General Situation of Working Face. Taking the 8003 working face of a coal mine in Shanxi as an example, the coal seam thickness ranges from 94 to 104 meters and contains multiple interbedded gangues, which are extracted through layered mining. The ground elevation of the 8003 working face ranges from +925 to +945 meters, with an average coal seam thickness of 5.67 meters and a dip angle of −2° to −5° along the roadway. Within the range of 440 meters and 554 meters ahead of the return airway and roadway of 8003 comprehensive caving, there exist SF14 and SF15 normal faults. The geological conditions of the 8005 working face are similar to those of the 8003 working face, and rock burst and frequent mine tremors occurred during mining.

According to the indicators in Table 1, the FAHP criteria layer can be divided into the following levels First, the stability level of the goaf support layer, which includes indicators such as the distance between the hard and thick rock layers and the coal seam inside the overlying fracture zone, mining depth, and thickness of the remaining coal seam, is used to evaluate the stability of the goaf support layer. Second, the stability level of the working face, which includes indicators such as the historical number of occurrences of the same level of coal seam rock bursts, the ratio between the stress increment of the structure and the normal stress %, the uniaxial compressive strength/MPa, and the elasticity index are used to evaluate the stability of the working face. Third, the level of mining technology, which includes indicators such as the working face length, the width of the segment coal pillar, and the relationship between the working face and the adjacent goaf, is used to evaluate the rationality, efficiency, and safety of mining technology. Therefore, the basic parameters of the 8003 working face are entered in Table 1, and the CF-TOPSIS evaluation model is employed to predict its rock burst hazard.

3.2. Comprehensive Weighting Prediction and Rock Burst Hazard Assessment. Table 1 is imported into the improved CRITIC objective weighting model and then substituted into equation (7) together with the subjective weight obtained by FAHP, which yields the ideal evaluation index for rock burst factor assessment, as presented in Table 2.

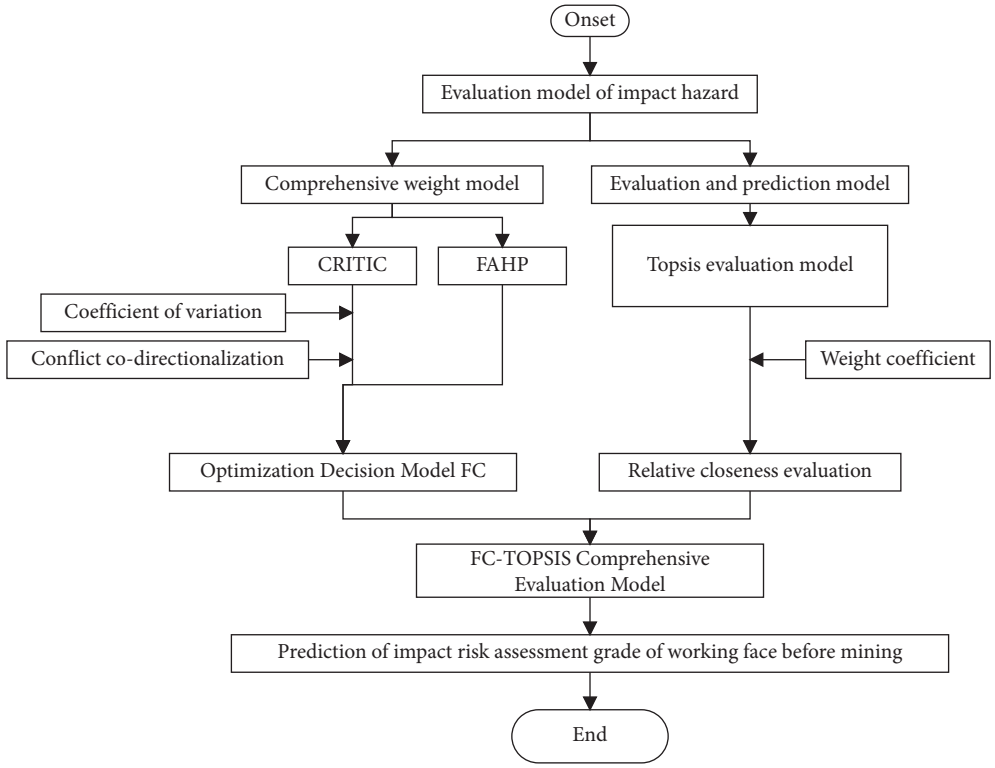

Figure 1: CF-TOPSIS comprehensive evaluation model.

Table 1: Evaluation criterion system of rock burst grade.

Evaluating indicators	Weak	Mid	Strong	8003 working face
The same level of coal seam rock burst history times (times)	1	2	3	2
Mining depth h (m)	400	600	800	647
The distance d between the hard thick strata and the coal seam in the overlying fracture zone	100	50	20	15.85
Ratio of stress increment to normal stress in the mining area (%)	10	20	30	17.3
Uniaxial pressure resistance (MPa)	10	14	20	10.3
Elasticity index	2	3.5	5	1.58
Relationship between the working face and adjacent goaf	1 side goaf	2 side goaf	3 side goaf	1 side goaf
Working face length (m)	300	150	100	290
Section coal pillar width (m)	3	6	10	48
Bottom coal thickness (m)	0	1	2	0

Comparison of the weights in Table 1 reveals differences in the degree of influence of different rock burst criteria on rock burst events. Specifically, the relationship between the primary and secondary factors affecting rock burst is $A3 > A2 > A4 > A1$. This analysis is of significant value in guiding the optimal selection of rock burst criteria.

Equations (1)–(4) are utilized for the creation of a line chart showcasing index weights for the unoptimized CRITIC model. In order to optimize said model, the integration of equations (5) and (8) is carried out to obtain the optimal CRITIC objective weight. Once the optimized objective weight and the FAHP subjective weight w_{Bj} are substituted into equation (12), the weight curve is derived and compared with real-life conditions. Figure 2 is obtained by comparing the outcomes of the unoptimized and optimized CRITIC models with the optimized CRITIC + FAHP model.

Through comparison of weight values before and after optimization, as illustrated in Figure 2, slight increases in the weight values of indicators $A2$, $A4$, and $A5$ are observed after FAHP optimization, while the weight of indicator $A3$ decreases slightly. The CF weight evaluation model enables a more reasonable weight index to be applied that aligns with actual site conditions, surmounting limitations encountered by conventional models that exhibit significant differences. Verification of the optimized results through field analysis confirms their alignment with staff subjective evaluations.

In the comprehensive index method, rock burst events are categorized into four grades: no, weak, medium, and strong. Weak, medium, and strong critical values of rock burst correspond to $S1$, $S2$, and $S3$, respectively, with the value of S representing the working surface value to be measured. When $S < S1$, there is no rock burst hazard, and

Table 2: Subjective and objective weight and comprehensive weight index.

Influencing factors	Subjective weight FAHP	Objective weight CRITIC	Combined weight CF
$A1$	0.0936	0.0613	0.0940
$A2$	0.0923	0.0771	0.1045
$A3$	0.1028	0.2844	0.2167
$A4$	0.1360	0.0520	0.1015
$A5$	0.1165	0.0822	0.0883
$A6$	0.1164	0.0903	0.0882
$A7$	0.0865	0.0866	0.0761
$A8$	0.0864	0.0828	0.0757
$A9$	0.0893	0.0967	0.0817
$A10$	0.0802	0.0866	0.0733

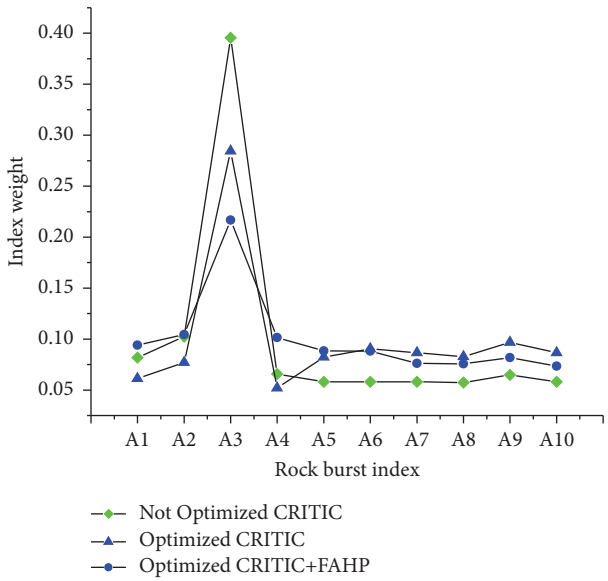

Figure 2: Optimized and unoptimized indicators.

when $S1 \le S < S2$, it indicates weak rock burst hazard. For values where $S2 \le S < S3$, it represents medium rock burst hazard, and for values where $S3 \le S$, it represents strong rock burst hazard.

The CRITIC method is conducted without the inclusion of the coefficient of the variation method and the conflict forward optimization method. Furthermore, the total ranking of the TOPSIS hierarchy is not considered, and weight and equation (17) with w_{AB} are not added. The obtained TOPSIS model is unoptimized, as illustrated in Figure 3(a). Subsequently, a comprehensive evaluation model is established by combining FAHP with the unoptimized TOPSIS model, as depicted in Figure 3(b). Ultimately, the comprehensive evaluation results for the CF-TOPSIS model are presented in Figure 3(c).

Figure 3(a) shows that the comprehensive evaluation index of traditional CRITIC and traditional TOPSIS methods for rock burst is $w = (0, 0.3933, 1,$ and $0.5807)$ and that the evaluation grade of the rock burst index is medium. In contrast, Figure 3(b) shows that, with the combination of FAHP and unoptimized TOPSIS, the evaluation index of rock burst is weak and $w = (0, 0.4594, 1,$ and $0.2056)$. Both models exist, and when $S < S1$, it is difficult to accurately predict the hazard of rock burst in the working face to be measured, since the index cannot be negative. Moreover, only when $S = 1$, a strong level of rock burst can be determined. Therefore, the critical value interval of traditional models has certain limitations.

The CF-TOPSIS evaluation model produces an evaluation index of $w = (0.0569, 0.3638, 0.8360,$ and $0.5352)$, which is medium in 8003 coal mine conditions. When no rock burst danger exists, the result of the working face prediction indicates no rock burst hazards when $w < 0.0569$. Conversely, when $w \ge 0.8360$, a strong rock burst hazard is predicted, as shown in Figure 3(c). This method is only suitable for research at coal mine experimental sites, and there may be some special conditions or factors at other sites that may not be applicable to other sites. Therefore, this method cannot simply be applied to other sites and needs to be adapted and improved according to the specific situation.

3.3. Prediction of Rock Burst under Microseismic Monitoring Technology. The process of microseismic event evolution, from a dispersed pattern in space to self-organized concentration, is a distinct characteristic of rock burst precursors. The energy level of a single event per day is classified as moderate hazard, ranging between 10^4–10^6 J, with the potential for a strong rock burst hazard exceeding 10^6 J.

Based on the microseismic monitoring data obtained from the 8003 working face, as illustrated in Figures 4 and 5, the majority of microseismic events recorded near the working face possessed an energy range of 10^4–10^6 J, which accounted for 88% of the total events within the considered time period. The weaker events with energy levels below 10^4 J comprised 11.75% of the total events observed. There was only one instance of a microseism event with an energy level exceeding 10^6 J, which occurred during directional blasting for decompression in the roadway at the site. Consequently, based on a comprehensive assessment, the rock burst hazard level for the 8003 working face can be classified as medium.

3.4. Characteristic Analysis of Large Energy Signals. The coal mine in Shanxi, China, has a mining depth ranging from +925 to +945 meters. As multistage large-scale mining methods are employed and mining depth deepens, safety hazards such as rock burst become increasingly prominent. To ensure mine safety, an independently developed microseismic monitoring system with a sensor sampling frequency of 2000 Hz is installed in the mine. During the safety monitoring process, significant energy microseismic events are detected. Through eliminating irrelevant interference signals, the collected on-site microseismic signals, coupled with large energy vibration signals, are analyzed as depicted in Figures 6 and 7.

It is evident from the decomposition results presented in Figure 8 that the frequency of the microseismic signal persists in the time domain. Additionally, the time-frequency diagram illustrated in Figure 9 reveals that the

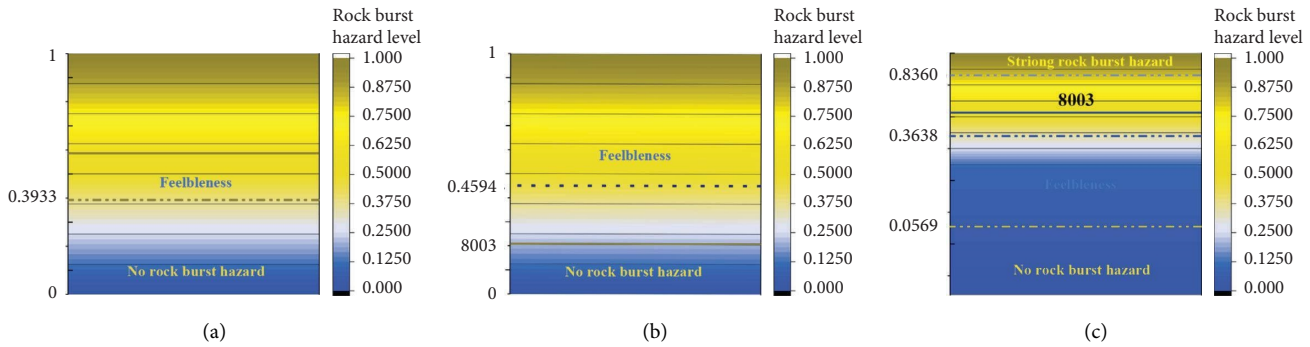

Figure 3: Evaluation index of rock burst (a–c).

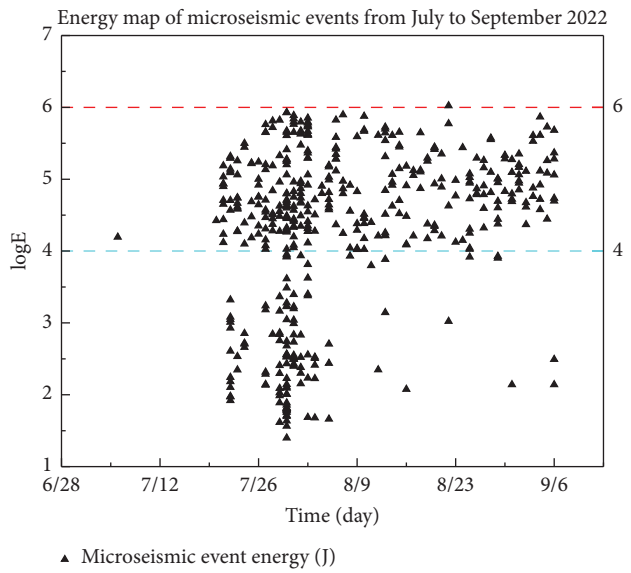

Figure 4: Energy map of microseismic events from July to September 2022.

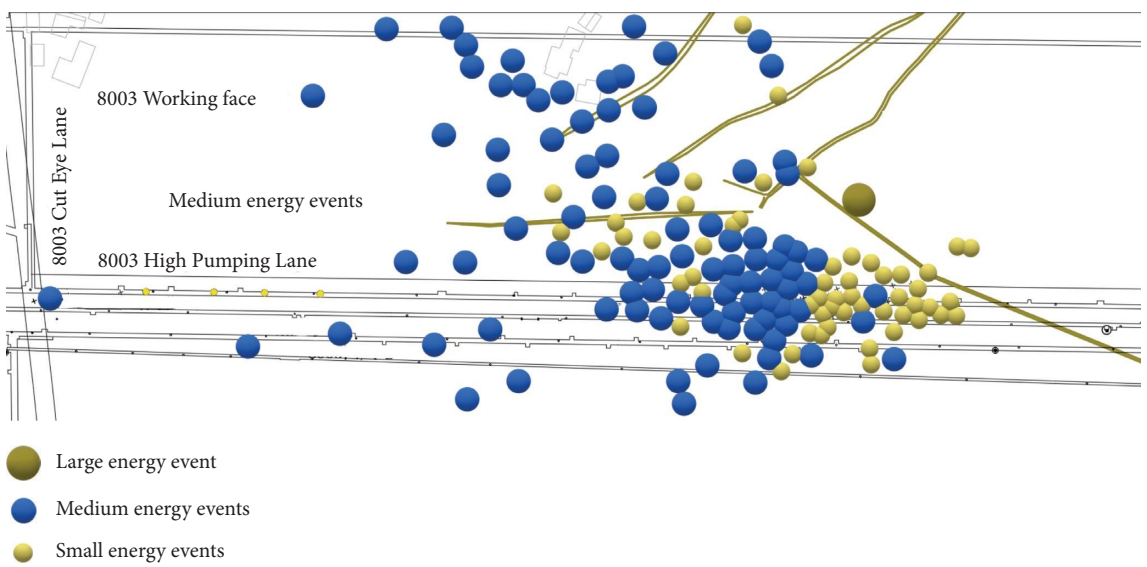

Figure 5: Microseismic event distribution map of the 8003 working face.

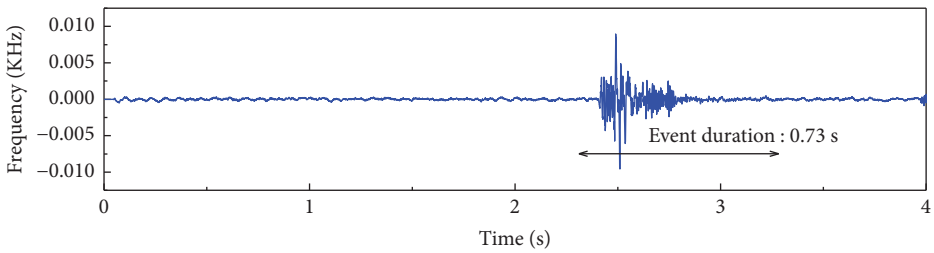

Figure 6: Microseismic signal waveform of rock mass.

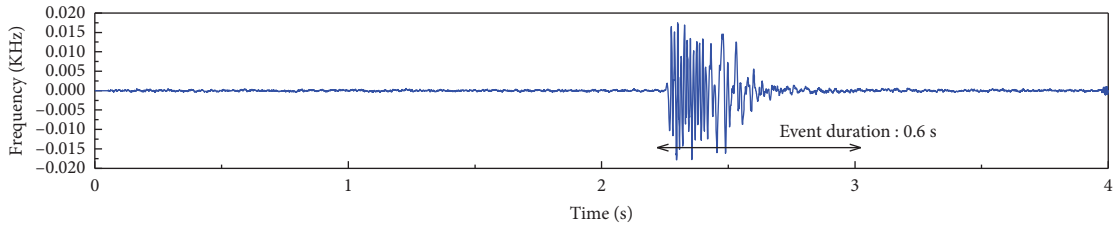

Figure 7: High energy microseismic signal waveform.

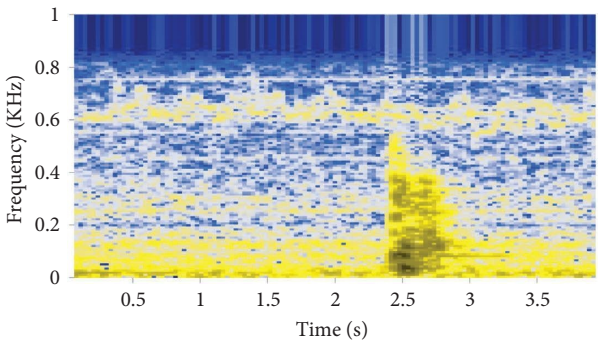

Figure 8: Time-frequency diagram of the rock microseismic signal.

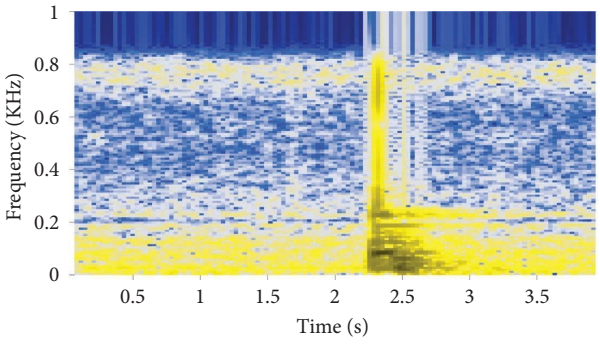

Figure 9: High energy microseismic signal waveform.

large energy signal displays traits such as short time duration, discontinuity, and high frequency. These attributes are indicative of a typical blasting signal. It is noteworthy to remark that the findings presented in this study provide valuable insights into the characteristics of microseismic signals, which can be leveraged for optimizing blasting processes and enhancing safety measures in mining operations. From the perspective of a trigger mechanism, microseismic events are the release of rock accumulated energy, and the process is relatively slow, mostly in the form of shear failure [37–39]. The blasting signal mainly produces longitudinal waves, with strong energy and fast attenuation, which is a typical rock burst response [40–43]. Therefore, it is preliminarily judged that the large energy signal is a blasting signal. Through subsequent field verification, it is further confirmed that the large energy signal is a blasting signal [44].

3.5. Drill Cutting Method. The current study focuses on the solid coal side of the 8003 working face and aims to determine and analyze the size of stress and the degree of rock burst danger. To achieve this, the pressure relief blasting method was utilized to measure the amount of pulverized coal (in kilograms) in the borehole. Additionally, the amount of drill cutting was measured at intervals of one meter, and the drill cutting absorption index was measured at intervals of two meters. If the measured amount of pulverized coal at the test site exceeds the critical value or the pressure of Δh_2 (drill cutting absorption index) exceeds 200 Pa, it indicates an increased hazard of rock burst occurrence. The actual and critical values of the cuttings absorption index are depicted in Figure 10.

The Δh_2 value serves as a comprehensive indicator of the coal damage degree. To obtain this value, it is necessary to extract drill cuttings at predetermined locations and subsequently sieve them with apertures of 1 mm and 3 mm before transferring the resultant particles to the coal sample bottle. After waiting for 3 minutes from the time of particle generation to sampling, the coal sample bottle is started. The absorption reading, recorded 2 minutes thereafter, equates to the Δh_2 value. The 8003 working face is subjected to measurement of an average of once every three days. Based on the August data analysis, 84% of the drill cuttings' absorption index was lower than the critical value of 200 MPa,

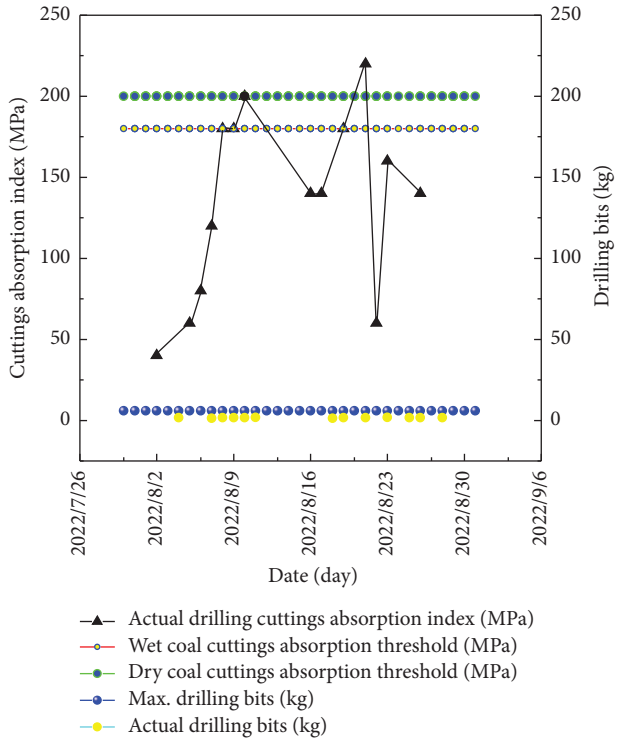

Figure 10: Drilling cuttings absorption index and drilling cuttings amount.

while 16% of the drill cutting absorption index (200 MPa on August 9th and 220 MPa on August 22nd) reached the critical absorption index value, necessitating further attention and assessment. Subsequent testing revealed that the actual drill cuttings did not achieve peak values on August 9th and August 22nd. As such, it was concluded that there was no imminent hazard of strong rock bursts. Overall, the 8003 working face poses a rock burst hazard.

4. Conclusion

(1) The present study proposes the CF-TOPSIS model for predicting rock burst hazard. To avoid any bias resulting from a single model, FAHP and CRITIC weight models are employed to determine the weight of rock burst factors. By incorporating the TOPSIS prediction model, the CF-TOPSIS prediction model for rock burst is obtained.

(2) The optimization of the traditional model is required to address its inadequacy in assessing the nonrock burst hazard phenomenon under rock burst conditions. Additionally, there is a need for enhanced accuracy in predicting the rock burst hazard associated with the working face being measured. Furthermore, it is important to compare the moderate rock burst hazard with the traditional model.

(3) The combination weighting method was utilized to obtain the total ranking of the CF evaluation index, revealing that distinct rock burst criteria exert varying degrees of influence on rock burst. The primary and secondary factors influencing the rock burst of the 8003 working face were determined as follows: the distance between the hard and thick strata in the overlying fractured zone and the coal seam ($A3$) possesses the greatest impact, followed by mining depth ($A2$), the ratio of stress increment to normal stress in the mining area ($A4$), and the number of rock bursts in the same horizontal coal seam ($A1$).

(4) This study examines the factors influencing rock burst from multiple perspectives, optimizes the traditional critical value interval, and proposes an effective prediction method for rock burst. Field practice is used to verify the feasibility and accuracy of this method, offering a novel approach to rock burst prediction.

Data Availability

All data generated or analyzed during this study are included within this article.

Disclosure

Feng Zhu and Haowei Song are the co-first authors.

Conflicts of Interest

The authors declare that there are no conflicts of interest regarding the publication of this paper.

Authors' Contributions

Feng Zhu and Haowei Song contributed equally to this work.

Acknowledgments

This work was partly supported by the Jining Key Research and Development Program Project (Grant no. 2021AQGX001), the Shandong Province Natural Science Foundation Key Project (Grant no. ZR2020KC012), the Shandong Province Deep Rock Bust Disaster Assessment Engineering Laboratory Open Project (Grant No. LMYK-2021-010), and the Jinan City "New 20 High Schools" Funding Project (Grant no. 2021GXRC037).

References

[1] K. C. Xie, W. Y. Li, and W. Zhao, "Coal chemical industry and its sustainable development in China," *Energy*, vol. 35, no. 11, pp. 4349–4355, 2010.

[2] X. B. Li, F. Q. Gong, M. Tao et al., "Failure mechanism and coupled static-dynamic loading theory in deep hard rock mining: a review," *Journal of Rock Mechanics and Geotechnical Engineering*, vol. 9, no. 4, pp. 767–782, 2017.

[3] H. Wang, M. Li, and X. F. Shang, "Current developments on micro-seismic data processing," *Journal of Natural Gas Science and Engineering*, vol. 32, pp. 521–537, 2016.

[4] F. F. Zhang, "Analysis on the difference of energy evolution in the process of energy storage failure of strong coal rush rock samples under different adaptive modification regulation

measures," *Shock and Vibration*, vol. 2022, Article ID 1471945, 11 pages, 2022.

[5] S. Di, "Research on the source mechanism and source prevention and control system of deep rock burst," *Advances in Civil Engineering*, vol. 2020, Article ID 8881759, 9 pages, 2020.

[6] Z. Z. Jia, Z. L. Song, J. F. Fan, and J. Y. Jiang, "Prediction of blasting fragmentation based on GWO-ELM," *Shock and Vibration*, vol. 2022, Article ID 7385456, 8 pages, 2022.

[7] C. M. Zheng, J. Y. Zheng, X. J. Peng, and L. Zhou, "Study on failure characteristics and rock burst mechanism of roadway roof under cyclic dynamic load," *Shock and Vibration*, vol. 2021, Article ID 7074350, 11 pages, 2021.

[8] X. J. Chen, L. Y. Li, and L. Wang, "The mechanical effect of typical dynamic disaster evolution and occurrence in coal mines," *Energy Sources, Part A: Recovery, Utilization, and Environmental Effects*, vol. 44, no. 2, pp. 2839–2850, 2022.

[9] L. J. Dong, X. B. Li, and K. Peng, "Prediction of rockburst classification using Random Forest," *Transactions of Nonferrous Metals Society of China*, vol. 23, no. 2, pp. 472–477, 2013.

[10] J. Zhou, X. B. Li, and H. S. Mitri, "Evaluation method of rockburst: state-of-the-art literature review," *Tunnelling and Underground Space Technology*, vol. 81, pp. 632–659, 2018.

[11] S. C. Wu, Z. G. Wu, and C. X. Zhang, "Rock burst prediction probability model based on case analysis," *Tunnelling and Underground Space Technology*, vol. 93, Article ID 103069, 2019.

[12] F. X. Jiang, Y. Feng, and Y. Liu, "Study on dynamic assessment method of impact risk before stope return," *Journal of Rock Mechanics and Geotechnical Engineering*, vol. 33, no. 10, pp. 2101–2106, 2014.

[13] F. Zhu and H. W. Zhang, "AHP +entropy weight method' based CW-TOPSIS model for predicting rock burst," *China Safety Science Journal*, vol. 27, no. 1, pp. 128–133, 2017.

[14] K. Han, J. Jin, M. Maia, J. Lowe, M. A. Sersch, and D. E. Allison, "Lower exposure and faster clearance of bevacizumab in gastric cancer and the impact of patient variables: analysis of individual data from AVAGAST phase III trial," *The AAPS Journal*, vol. 16, no. 5, pp. 1056–1063, 2014.

[15] G. B. Chen, "Comprehensive evaluation of rock burst risk based on cloud model and D-S theory," *Mining Research and Development*, vol. 37, no. 6, pp. 26–30, 2017.

[16] W. Cai, L. M. Dou, Z. L. Li, S. Y. Gong, and J. He, "Microseismic multidimensional information identification and spatio-temporal forecasting of rock burst:A case study of Yima Yuejin coal mine, Henan, China," *Chinese Journal of Geophysics*, vol. 57, no. 8, pp. 2687–2700, 2014.

[17] F. B. Meng, S. L. Jing, X. Z. Sun, C. X. Wang, Y. B. Liang, and D. Pang, "A new approach of disaster forecasting based on least square optimized neural network," *Geofluids*, vol. 2020, Article ID 8882241, 7 pages, 2020.

[18] M. A. Vukelic and E. N. Miranda, "Neural networks in petroleum engineering: a case study," *International Journal of Neural Systems*, vol. 7, no. 2, pp. 187–194, 1996.

[19] H. B. Zhao, B. R. Chen, and C. X. Zhu, "Decision tree model for rockburst prediction based on microseismic monitoring," *Advances in Civil Engineering*, vol. 2021, Article ID 8818052, 14 pages, 2021.

[20] E. Ghasemi, H. Gholizadeh, and A. C. Adoko, "Evaluation of rockburst occurrence and intensity in underground structures using decision tree approach," *Engineering with Computers*, vol. 36, no. 1, pp. 213–225, 2020.

[21] Y. Y. Pu, D. B. Apel, V. Liu, and H. Mitri, "Machine learning methods for rockburst prediction-state-of-the-art review," *International Journal of Mining Science and Technology*, vol. 29, no. 4, pp. 565–570, 2019.

[22] S. H. Yan, Y. Zhang, X. X. Liu, and R. Liu, "Rock burst intensity classification prediction model based on a bayesian hyperparameter optimization support vector machine," *Mathematics*, vol. 10, no. 18, p. 3276, 2022.

[23] X. B. Xie, W. Jiang, and J. Guo, "Research on rockburst prediction classification based on GA-XGB model," *IEEE Access*, vol. 9, pp. 83993–84020, 2021.

[24] Y. Y. Pu, D. B. Apel, and H. W. Xu, "Rockburst prediction in kimberlite with unsupervised learning method and support vector classifier," *Tunnelling and Underground Space Technology*, vol. 90, pp. 12–18, Aug. 2019.

[25] R. Liu, Y. C. Ye, N. Y. Hu, H. Chen, and X. H. Wang, "Classified prediction model of rockburst using rough sets-normal cloud," *Neural Computing & Applications*, vol. 31, no. 12, pp. 8185–8193, Dec. 2019.

[26] M. W. Wang, Q. Y. Liu, X. Wang, F. Q. Shen, and J. Jin, "Prediction of rockburst based on multidimensional connection cloud model and set pair analysis," *International Journal of Geomechanics*, vol. 20, no. 1, 2020.

[27] S. Afraei, K. Shahriar, and S. H. Madani, "Developing intelligent classification models for rock burst prediction after recognizing significant predictor variables, Section 1: literature review and data preprocessing procedure," *Tunnelling and Underground Space Technology*, vol. 83, pp. 324–353, 2019.

[28] E. Adar, B. Karatop, M. İnce, and M. S. Bilgili, "Comparison of methods for sustainable energy management with sewage sludge in Turkey based on SWOT-FAHP analysis," *Renewable and Sustainable Energy Reviews*, vol. 62, pp. 429–440, Sep. 2016.

[29] A. R. Krishnan, M. M. Kasim, R. Hamid, and M. Ghazali, "A modified CRITIC method to estimate the objective weights of decision criteria," *Symmetry*, vol. 13, no. 6, p. 973, 2021.

[30] S. Li, Y. H. Yan, J. Ren, Y. Z. Zhou, and Y. X. Zhang, "A sample-efficient actor-critic algorithm for recommendation diversification," *Chinese Journal of Electronics*, vol. 29, no. 1, pp. 89–96, 2020.

[31] L. J. Zhang and Z. Xiao, "Weighted clustering method based on improved CRITIC method," *Statistics & Decisions*, vol. 22, pp. 65–68, 2015.

[32] H. S. Zhao, J. X. Li, Z. Q. Mi, L. Pu, and Y. Y. Cui, "Grading evaluation of power quality based on CRITIC and improved Grey-TOPSIS," *Power System Protection and Control*, vol. 50, no. 3, pp. 1–8, 2022.

[33] Z. Wei, "Aquifer water abundance evaluation using a fuzzy-comprehensive weighting method," *IOP Conference Series: Earth and Environmental Science*, vol. 39, 2016.

[34] Z. Zhang, Y. Y. Wang, and Z. X. Wang, "A grey TOPSIS method based on weighted relational coefficient," *Journal of Grey System*, vol. 26, no. 2, pp. 112–123, 2014.

[35] Z. S. Tan, H. Lai, Z. L. Li et al., "Research on the tunnel boring machine selection decision-making model based on the fuzzy evaluation method," *Applied Sciences*, vol. 12, no. 21, Article ID 10802, 2022.

[36] R. M. Czekster, T. Webber, A. H. Jandrey, and C. A. M. Marcon, "Selection of enterprise resource planning software using analytic hierarchy process," *Enterprise Information Systems*, vol. 13, no. 6, pp. 895–915, 2019.

[37] S. Q. He, D. Z. Song, H. Mitri et al., "Integrated rockburst early warning model based on fuzzy comprehensive evaluation method," *International Journal of Rock Mechanics and Mining Sciences*, vol. 142, Article ID 104767, 2021.

[38] L. Huang, J. Li, H. Hao, and X. Li, "Micro-seismic event detection and location in underground mines by using Convolutional Neural Networks (CNN) and deep learning," *Tunnelling and Underground Space Technology*, vol. 81, pp. 265–276, 2018.

[39] Y. Y. Di and E. Y. Wang, "Rock burst precursor electromagnetic radiation signal recognition method and early warning application based on recurrent neural networks," *Rock Mechanics and Rock Engineering*, vol. 54, no. 3, pp. 1449–1461, 2021.

[40] R. S. Jia, T. B. Zhao, H. M. Sun, and X. H. Yan, "Micro-seismic signal denoising method based on empirical mode decomposition and independent component analysis," *Chinese Journal of Geophysics*, vol. 58, no. 3, pp. 1013–1023, 2015.

[41] C. W. Li, X. Y. Sun, C. Wang, X. M. Xu, B. J. Xie, and J. Li, "The correlated characteristics of micro-seismic and electromagnetic radiation signals on a deep blasting workface," *Journal of Geophysics and Engineering*, vol. 13, no. 6, pp. 1020–1035, 2016.

[42] B. L. Li, N. L. Li, E. Y. Wang, X. L. Li, Y. Niu, and X. Zhang, "Characteristics of coal mining microseismic and blasting signals at Qianqiu coal mine," *Environmental Earth Sciences*, vol. 76, no. 21, p. 722, 2017.

[43] B. L. Li, N. Li, E. Y. Wang et al., "Discriminant model of coal mining microseismic and blasting signals based on waveform characteristics," *Shock and Vibration*, vol. 2017, pp. 1–13, 2017.

[44] D. V. Ghica, B. Grecu, M. Popa, and M. Radulian, "Identification of blasting sources in the Dobrogea seismogenic region, Romania using seismo-acoustic signals," *Physics and Chemistry of the Earth*, vol. 95, pp. 125–134, 2016.